Title
OPERATION OF HYDROGEN BUBBLE CHAMBERS IN HIGH-ENERGY PHOTON BEAMS

Permalink
https://escholarship.org/uc/item/18c000pw

Authors
Gates, Duane C.
Kenney, Robert W.
McPherson, Donald A.
et al.

Publication Date
1959-10-08

UCRL 8934

UNIVERSITY OF CALIFORNIA

Ernest O. Lawrence Radiation Laboratory

BERKELEY, CALIFORNIA

for pub. RSI

UCRL-8934

UNIVERSITY OF CALIFORNIA

Lawrence Radiation Laboratory
University of California
Berkeley, California

Contract No. W-7405-eng-48

OPERATION OF HYDROGEN BUBBLE CHAMBERS IN HIGH-ENERGY PHOTON BEAMS

Duane C. Gates, Robert W. Kenney, Donald A. McPherson,
and William P. Swanson

October 8, 1959

Printed for the U. S. Atomic Energy Commission

OPERATION OF HYDROGEN BUBBLE CHAMBERS IN HIGH-ENERGY PHOTON BEAMS

Duane C. Gates, Robert W. Kenney, Donald A. McPherson,
and William P. Swanson

Lawrence Radiation Laboratory
University of California
Berkeley, California

October 8, 1959

ABSTRACT

Operation of the Alvarez 4-inch hydrogen bubble chamber in a high-energy photon beam is described, the techniques employed in several modes of operation are discussed, and the corresponding bubble chamber conditions are tabulated. Reduction of electron background was accomplished by beam hardening and by using a Mylar beam-entrance window on the chamber.

OPERATION OF HYDROGEN BUBBLE CHAMBERS IN HIGH-ENERGY PHOTON BEAMS*

Duane C. Gates, Robert W. Kenney, Donald A. McPherson,
and William P. Swanson

Lawrence Radiation Laboratory
University of California
Berkeley, California

October 8, 1959

I. INTRODUCTION

The development of hydrogen bubble chambers at this laboratory has been carried on by Prof. Luis W. Alvarez and his group, and their physics program for the various chambers has been largely oriented toward the Bevatron. We have applied the Alvarez 4-inch-diameter hydrogen bubble chamber to problems of photon interactions at the Berkeley synchrotron, and have made extensive use of Professor Alvarez's apparatus and basic techniques. Thin low-Z beam windows on the chamber were required to reduce electron background and make operation of the chamber in a high-energy photon beam feasible. This note concerns the window modifications and the problems peculiar to the use of a bubble chamber in the photon beam from an electron accelerator.

John M. Teem and David Alyea (California Institute of Technology) first showed that a hydrogen bubble chamber could be operated successfully in a high-energy photon beam by placing the unmodified Alvarez 4-in. chamber in the Berkeley synchrotron beam and obtaining photographs of photopions and electron pairs from hydrogen. These investigators determined electron energies by measuring curvatures of the tracks in a pulsed 10-kilogauss field applied to the chamber. Observations were difficult because the tracks were partially obscured in excessive electron background from

---

*Work done under the auspices of the U. S. Atomic Energy Commission.

the thin stainless steel beam-entrance window. Somewhat later, the authors, and independently Donald H. Miller and David A. Hill at General Electric Company Research Laboratory, used bubble chambers equipped with very thin, low-Z beam windows to study photon reactions in hydrogen and deuterium.[1]

II. APPARATUS AND PROCEDURE

The major problem in operating a bubble chamber in a photon beam arises from the undesirable electron background produced in and near the chamber by Compton-recoil and pair-creation processes. In the investigations at Berkeley, the primary photon beam from the synchrotron was passed through the chamber as shown in Fig. 1.

The electron background from sources external to the hydrogen itself was reduced to a low level by sweeping all charged particles out of the photon beam after it entered the vacuum window (located as shown in Fig. 1), by providing open beam holes in the copper heat shield, and by providing thin entrance and exit windows on the bubble chamber.

The thin low-Z window which admits the pure photon beam into the interior of the bubble chamber is the most important modification of the original Alvarez chamber, and is essential to efficient operation in a photon beam. The bubble chamber wall is provided with a flange and double lead gasket for holding a 15/16-in.-diameter Mylar beam-entrance window of 0.0075-in.-thickness, which is the only source of charged-particle background with the exception of the hydrogen itself. Details are shown in Fig. 2, and are due to Miller and Hill. One Mylar window has sustained 300,000 chamber expansions with no apparent damage to the plastic. The 0.0075-in.-Mylar window has also withstood static pressure tests of 165 psia at 24° K, and also at room

---

[1] Donald H. Miller and David A. Hill, Threshold Photopion Production in Hydrogen, to be submitted to Physical Review.

temperature, without damage. Mylar windows of 7/8-in. diameter can be safely constructed of Mylar only 0.004-in. thick, but it was felt that the extra safety inherent in the thicker window was desirable, particularly since the electron background from the thicker window was only 15% of the electron production within the hydrogen itself. An exit window of 0.010-in. stainless steel was hard-soldered onto the bubble chamber wall, and an open beam hole in the exit face of the copper heat shield was provided to minimize the backward flux of heavy charged particles into the chamber from photo interactions in the chamber exit wall and in the neighboring heat shield. Figure 3 shows a typical flux of heavy particles arising from the thick exit wall of the unmodified bubble chamber, where the quantum limit energy of the incident bremsstrahlung was 340 Mev and the incident bremsstrahlung flux was 10^6 Mev. After the installation of the thin exit window, backward tracks arising from this source have been seen only extremely rarely.

Neutrons produced a negligibly small contribution to the background, measured by the observed recoil tracks originating in the chamber outside the region of the photon beam.

A. Beam Hardener

A major portion of the charged-particle background from a normal (unhardened) bremsstrahlung beam consisted of Compton electrons, which are produced principally by photons of energy less than 1 Mev. In order to decrease this background, the low-energy photon flux was selectively reduced by three orders of magnitude per 200-Mev photon by a photon beam hardener made of light elements (a column of LiH: 1/10 H_2O, 100 g/cm^2 in length). The high-energy Compton recoil background was reduced by a factor of 1.7 per 200-Mev photon. In all runs the bremsstrahlung beam from the synchrotron passed through the hardener before entering the bubble chamber. The spectrum transmitted by the hardener was determined by measuring the photon transmission of the hardener as a function of energy, using a standard pair-spectrometer absorption technique. The results of this measurement, shown in Fig. 4, were used to calculate the spectral shape of the hardened beam, assuming a Schiff bremsstrahlung spectrum incident upon the hardener. These spectra are shown in Fig. 5.

B. Chamber Alignment

The alignment of the bubble chamber in the photon beam was facilitated by a small lead fiducial point marking the center of the Mylar entrance window. The fiducial marker could be inserted or removed from outside the vacuum system. During the initial alignment procedure an x-ray photographic film was exposed by the photon beam behind the bubble chamber as shown in Fig. 1. The photographic image of the photon beam, with the outline of the lead fiducial marker superposed, allowed precise centering of the chamber Mylar entrance window in the beam. The fiducial mark was withdrawn upon completion of the alignment procedure. There was no evidence of electron production from interactions of the photon beam with the window flange, despite a radial clearance of only 1/16 in.

Typical freedom from incident electron background is shown in Fig. 6, where it is seen that six electrons arise within the chamber, and three from the entrance window itself.

III. PHOTON BEAM CHARACTERISTICS AND BUBBLE CHAMBER OPERATION

Two beam configurations have been used, (a) a large-diameter cylindrical beam, and (b) thin ribbon beam geometry viewed edgewise by the camera, each meeting the requirements of a different type of experiment. Table I gives details of beam geometries and the corresponding modes of operation of the bubble chamber.

When the production of electron triplets was being studied by observation of the three-body final state, the bubble chamber was operated at a temperature at which minimum-ionizing electrons left satisfactorily dense tracks. A large-diameter low-intensity photon beam was required so that the scanning efficiency for triplet events with very short recoil tracks would not be impaired by the presence of numerous background electrons. The maximum usable beam intensity was the relatively low value of 2.10^4 Mev/pulse for 340-Mev hardened bremsstrahlung, which gave a probability of 1/5 per picture for the production of a triplet with recoil of energy greater than 200 kev. Under these conditions the mean value of the ratio of triplets whose recoil energies exceeded 200 kev to all background tracks was 1/15. (See Table I.) Figure 6 shows a triplet event accompanied by typical electron background.

The chamber was filled with deuterium in order to observe the two reactions $\gamma + d \rightarrow \pi^+ + 2n$ and $\gamma + d \rightarrow \pi^- + 2p$ by positive-pion decay and by detecting the three-body charged final state, respectively. In the latter case very short tracks occur which must not be obscured by background. The cross section for pion production within 20 Mev of threshold is less by three orders of magnitude than that for electron production, so that practical counting-rate considerations require the observation of pion photoproduction in a high electron background. Satisfactory bubble chamber conditions were achieved by using a large-diameter hardened photon beam and by cooling the chamber to a temperature at which low-energy pions left conveniently dense tracks, but at which single electron tracks were so lightly ionizing that they were unrecognizable in a group of such tracks. Stable chamber temperature was required. (See Table I.) Figures 7 and 8 show typical examples of charged-pion photoproduction. That part of the chamber volume occupied by the photon beam was only partially obscured by the background of apparently uncorrelated single bubbles from the electrons produced by the photon beam. Nearly all electrons are directed forward, so that, in the absence of a magnetic field, the background of single bubbles remained within the beam volume, except for the tracks of those relatively few particles which were scattered out. The maximum usable beam intensity was determined by the highest density of single bubbles that would allow acceptable visibility of origins of events and short recoil tracks; this value, 10^6 Mev/pulse for 200-Mev hardened bremsstrahlung, gave a 1% probability per expansion of producing an observable $\pi^{\pm}$ of any energy within the chamber volume.

Miller and Hill (General Electric), and somewhat later the authors, have studied the reactions $\gamma + p \rightarrow \pi^+ + n$ and $\gamma + p \rightarrow \pi^0 + p$ in hydrogen bubble chambers exposed to high-intensity "ribbon" beams. In an effort to maximize the number of events per expansion, the photon beam was run at relatively high intensity, collimated to a ribbonlike geometry of small thickness, and viewed edge-on by the camera. Figure 9 shows an example of π^+ photoproduction and decay within the chamber. All tracks or portions of tracks lying in the region of the beam were obscured by the electron background; however, sufficiently sharp collimation of the photon beam was achieved (by means of a simple lead slit followed by one sweeping magnet) that the beam itself was restricted to a ribbonlike region of approximately 1/8-in. thickness with pion and proton tracks visible in the regions immediately adjacent to the beam. In this type of operation, the photon beam intensity was restricted to 2.10^7 Mev/pulse by the obscuration of portions of the bubble chamber adjacent to the beam by tracks of those electrons which are scattered out of the beam volume. This technique is highly satisfactory for investigating low-yield reactions, the products of which have ranges large compared with the projected beam width, because in this case the particle-range error is generally small enough so that the calculations of reaction kinematics are not subjected to undue uncertainties arising because the initial portion of the track is obscured by the beam itself. However, the technique is not applicable to the study of reactions that give rise to very short prongs, because of the complete obscuration of the origins of all photoproduction events.

ACKNOWLEDGMENTS

We are grateful to Professor A. C. Helmholz for his continued guidance and interest throughout the course of this work. To Professor Luis W. Alvarez and his group goes our grateful appreciation for the use of the bubble chamber and some of the data-analysis apparatus. The Mylar window design is due to Dr. D. Miller and Dr. D. Hill, and thanks are also due Dr. Miller for discussions and for his permission to quote some information prior to publication.

Table I

Bubble chamber operating conditions

	Experiment		
	Production of electron pairs and electron triplets from hydrogen	$\gamma + d \rightarrow \pi^- + 2p$ $\rightarrow \pi^+ + 2n$	$\gamma + p \rightarrow \pi^+ + n$
Beam geometry	Circular cross section 3/4 in. diam	Circular cross section 3/4 in. diam	Ribbon, 1/8×3/4 in.
Bubble chamber filling	Liquid hydrogen	Liquid deuterium	Liquid hydrogen
Magnetic field (kilogauss)	10 (pulsed Helmholtz coils)	0	0
Maximum usable beam intensity	Low intensity; 2:10^4 Mev per 340-Mev pulse	Medium intensity; 10^6 Mev per 200-Mev pulse	High intensity; 2:10^7 Mev per pulse at 200-Mev peak bremsstralung energy
Bubble chamber temperature (°K)	27.3±0.03 °K; 74±0.5 psig hydrogen vapor pressure; minimum-ionization tracks visible	31.7±0.04 °K; 90±0.5 psig deuterium vapor pressure; minimum-ionization tracks biased out	26.2±0.04 °K; 60±0.5 psig hydrogen vapor pressure; minimum-ionization tracks biased out
Bubble chamber pressure (psig)	95±5 before expansion; 43±5 at minimum	111±4 before expansion; 59±4 at minimum	90±5 before expansion; 38±5 at minimum
Remarks	Short prongs and origins of electromagnetic events visible within volume of photon beam.	Liquid deuterium density (expanded)= 0.127±0.0013 g/cm^3. Short prongs and origins of photopion events visible within volume of photon beam.	Entire volume of beam opaque; origins of π^+ obscured, but beam intensity high enough to produce large yield of usable events (1 per 20 expansions).

Figure Captions

Fig. 1. Schematic arrangement of apparatus.

Fig. 2. Mylar window. Gasket groove is cut 1/32 in. deep with 60-deg tool having a slightly rounded point.

Fig. 3. Charged particles from beam exit window in unmodified chamber.

Fig. 4. Photon transmission, T_{LiH} through LiH hardener versus the photon energy, k_{Mev}.

Fig. 5. Incident Schiff spectrum and spectrum transmitted by hardener. Here k is the photon energy in Mev, and n(k) is the number of photons, per Mev, of energy k.

Fig. 6. Electron triplet from hydrogen with typical electron background. Large-diameter low-intensity photon beam (see Table I).

Fig. 7. $\gamma + d \rightarrow \pi^- + 2p$; with large-diameter medium-intensity photon beam (see Table I). The longest track is the π^- - it leaves the chamber.

Fig. 8. $\gamma + d \rightarrow \pi^+ + 2n$; with large diameter medium-intensity photon-beam (see Table I). $\pi^+ - \mu^+ - e^+$ decays are also seen.

Fig. 9. $\gamma + p \rightarrow \pi^+ + n$; with high-intensity ribbon photon beam (see Table I). $\pi^+ - \mu^+$ decay is seen.

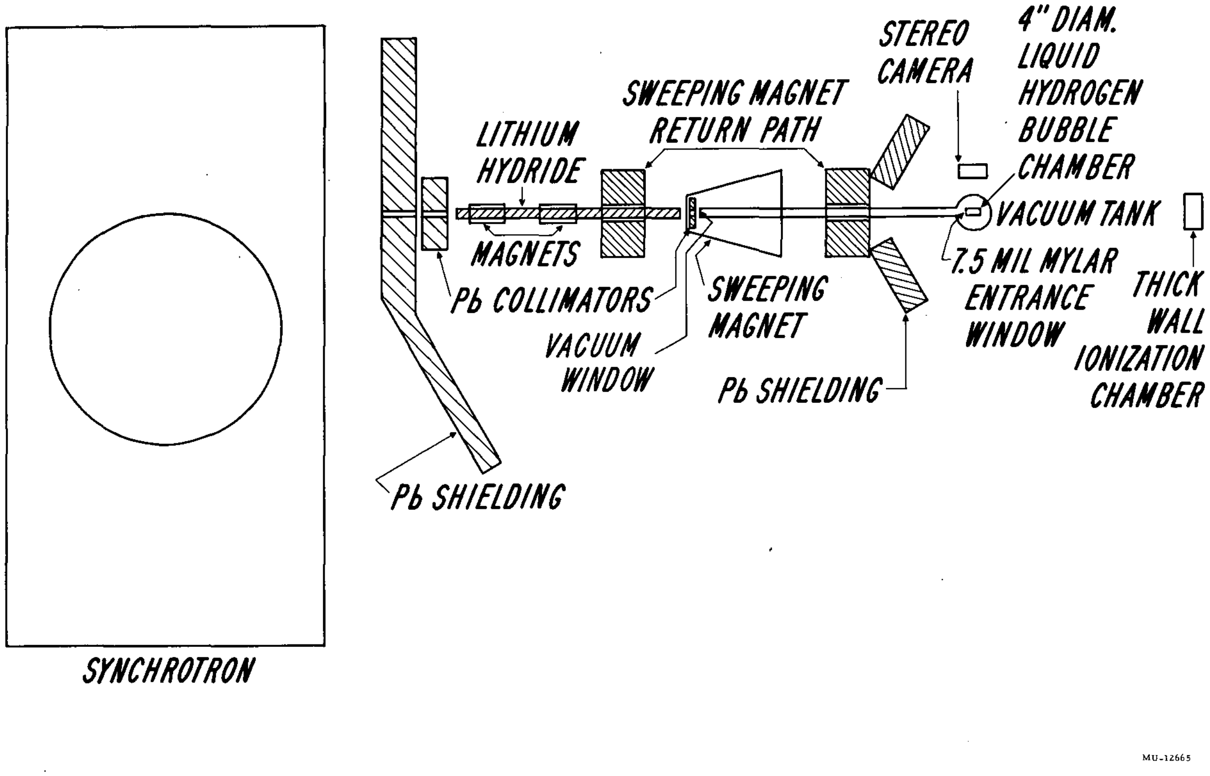
STEREO CAMERA
4" DIAM. LIQUID HYDROGEN BUBBLE CHAMBER
SWEEPING MAGNET RETURN PATH
LITHIUM HYDRIDE
VACUUM TANK
MAGNETS
7.5 MIL MYLAR ENTRANCE WINDOW
THICK WALL IONIZATION CHAMBER
Pb COLLIMATORS
SWEEPING MAGNET
VACUUM WINDOW
Pb SHIELDING
Pb SHIELDING
SYNCHROTRON
MU-12665

Fig. 1

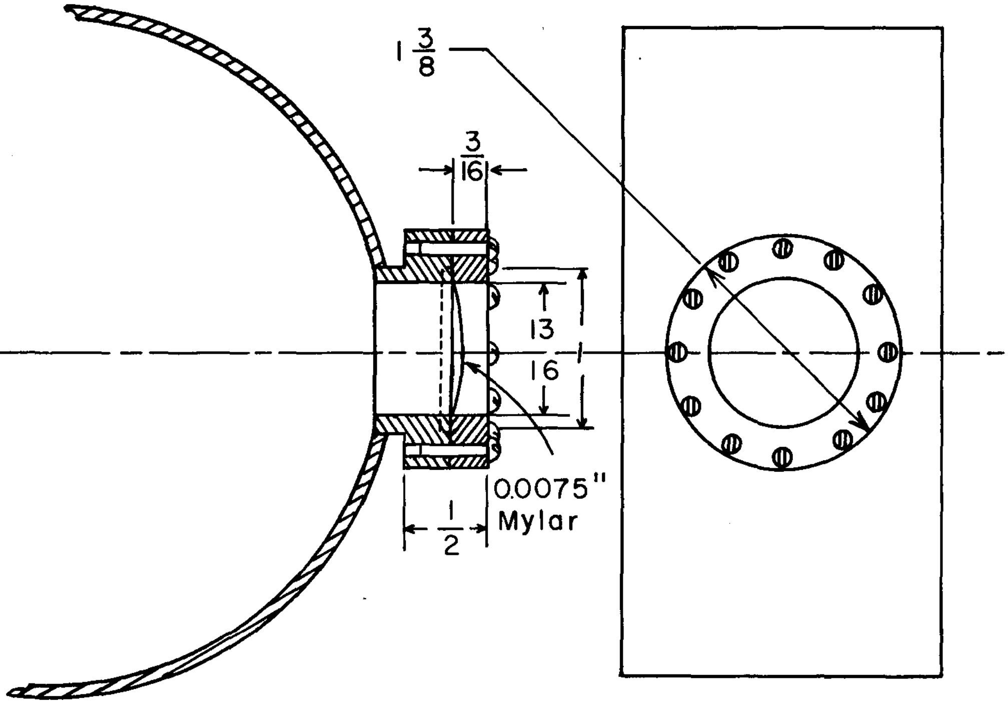

MU-18565

Fig. 2

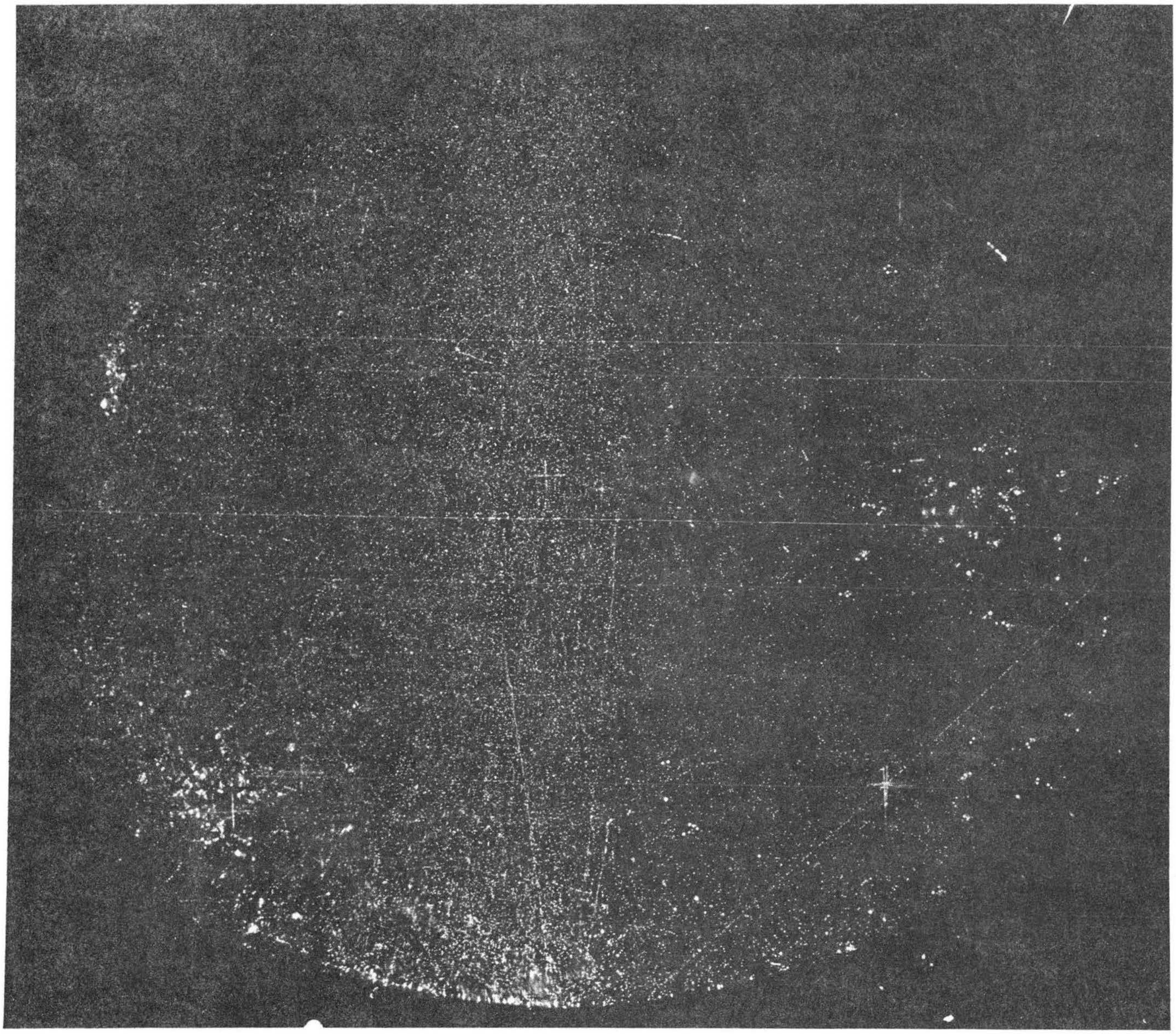

ZN-2271

Fig. 3.

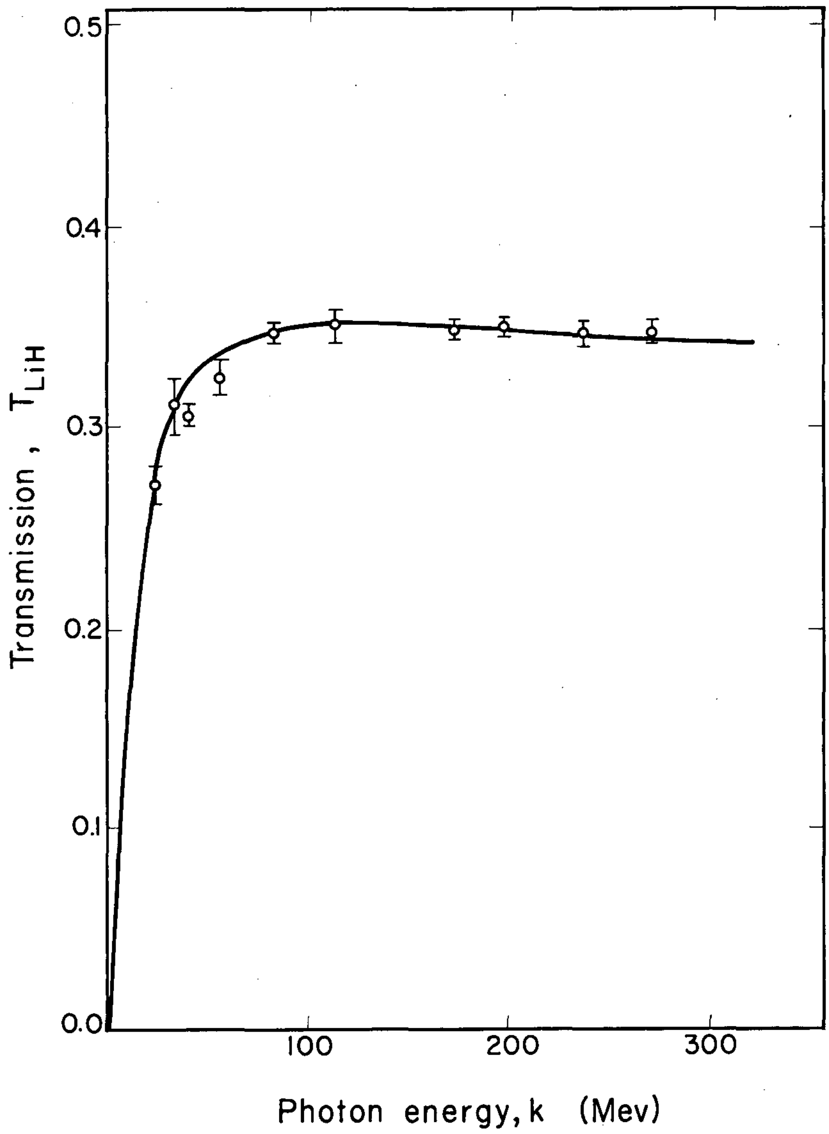

MU-18566

Fig. 4.

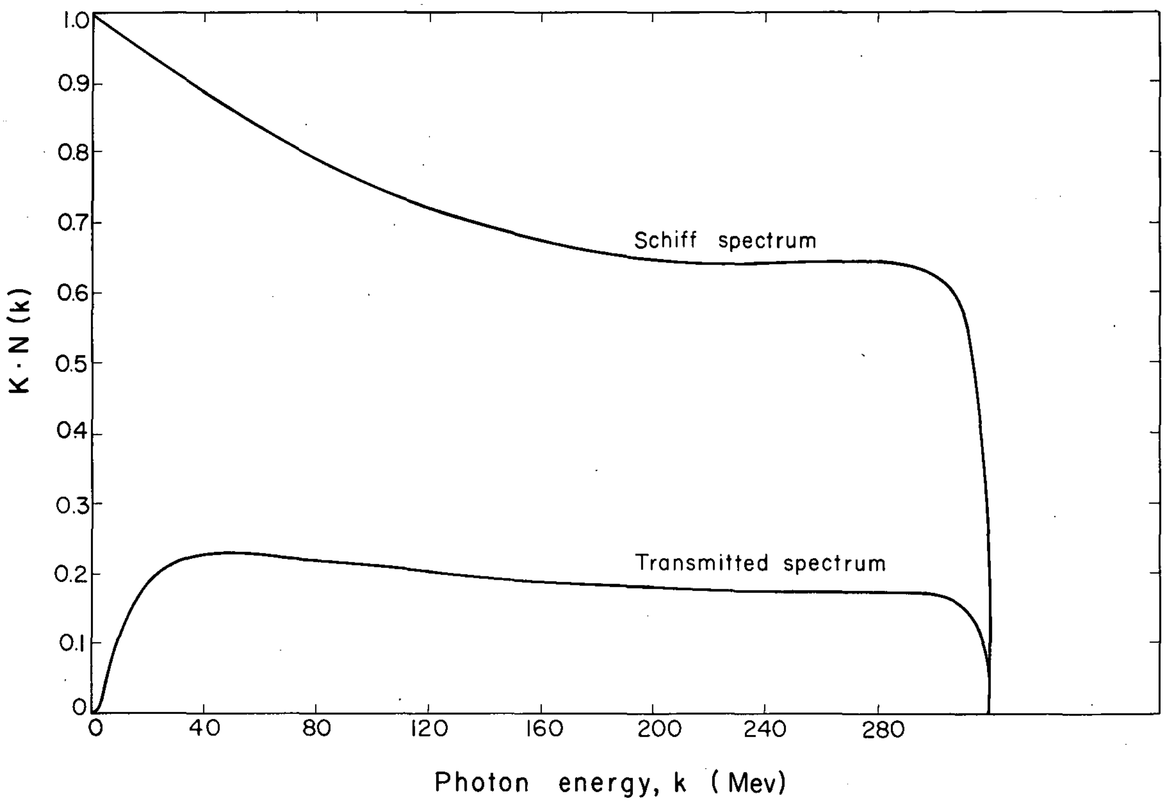

MU-18567

Fig. 5.

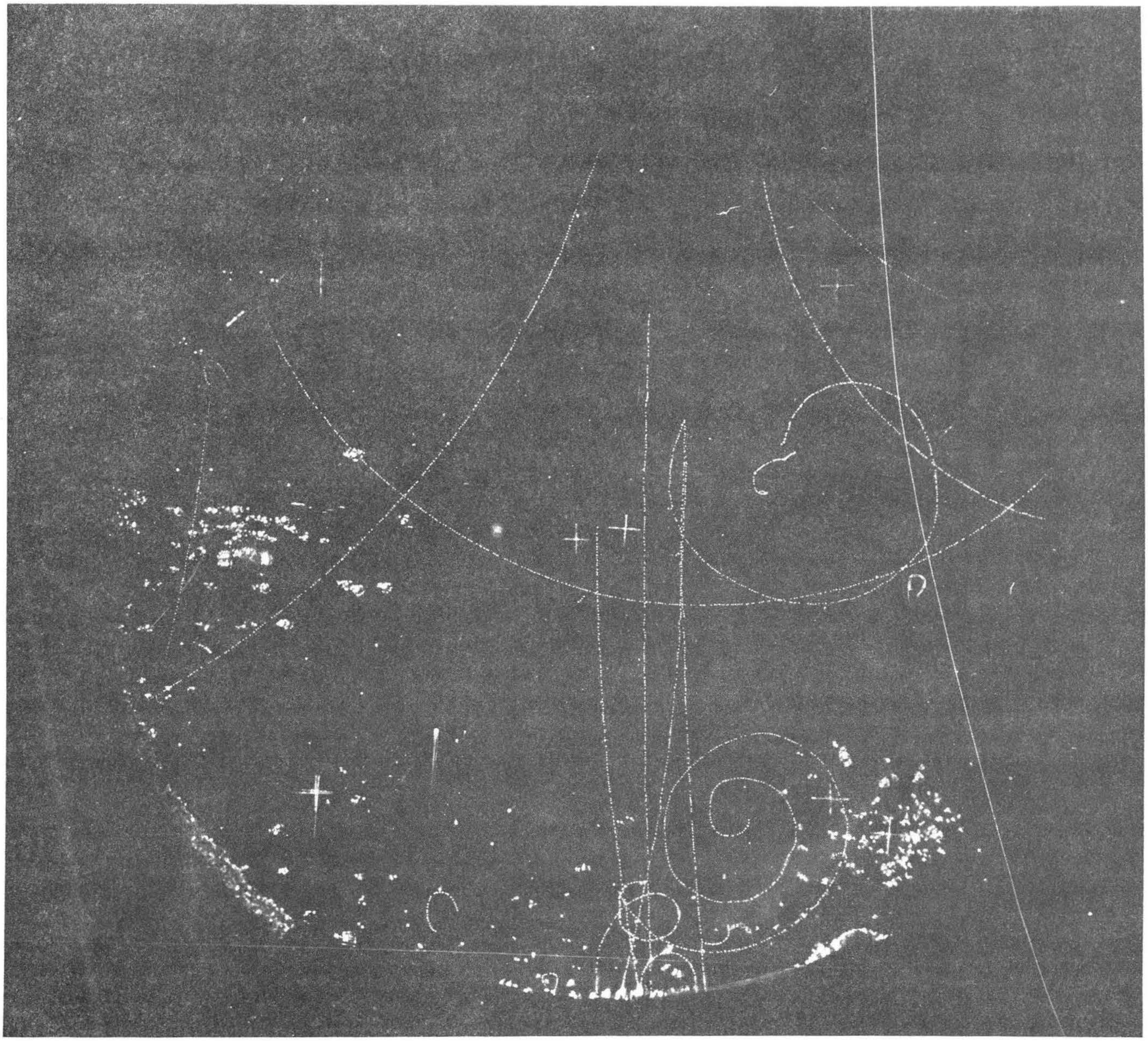

ZN-2272

Fig. 6

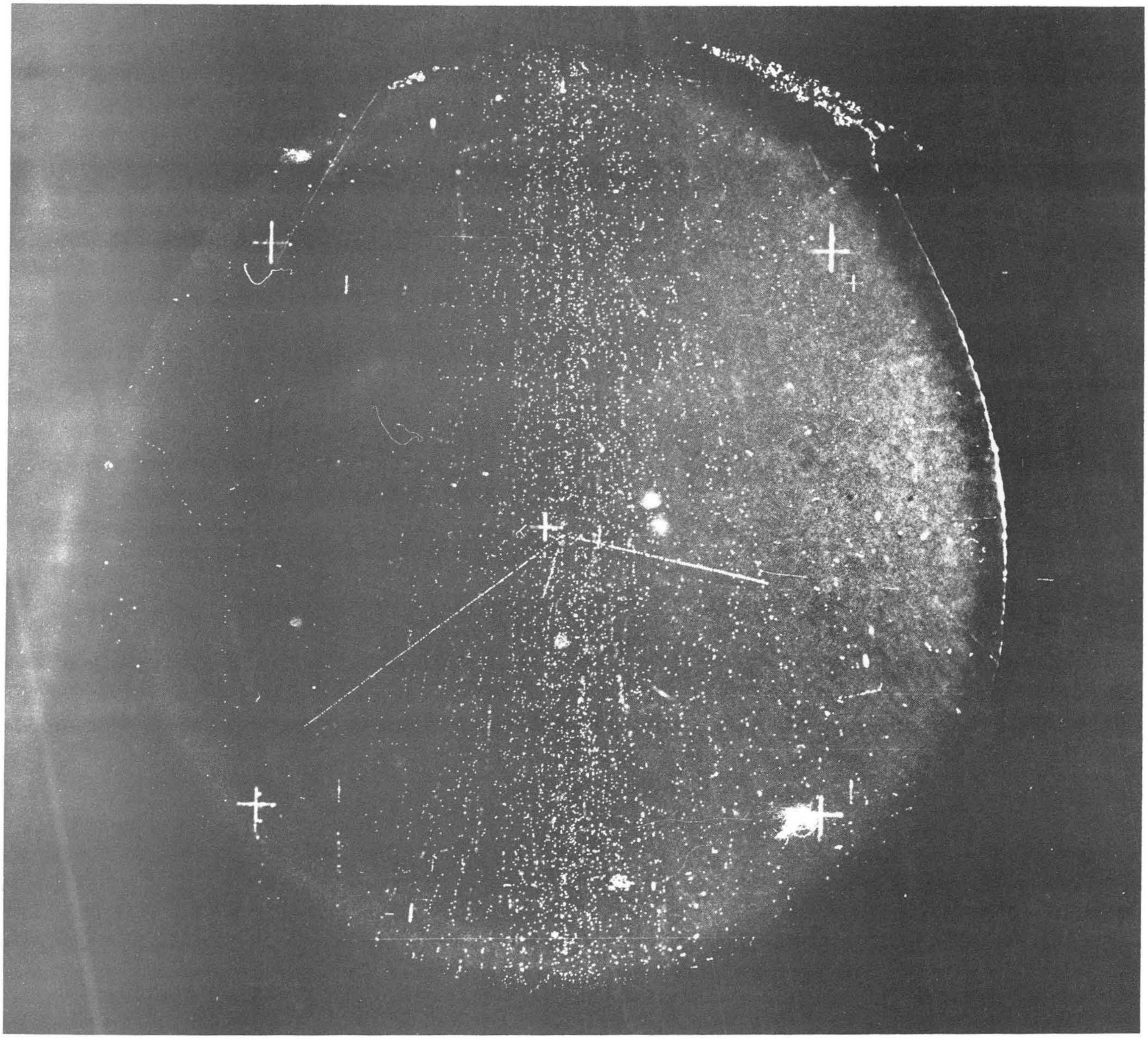

ZN-2273

Fig. 7.

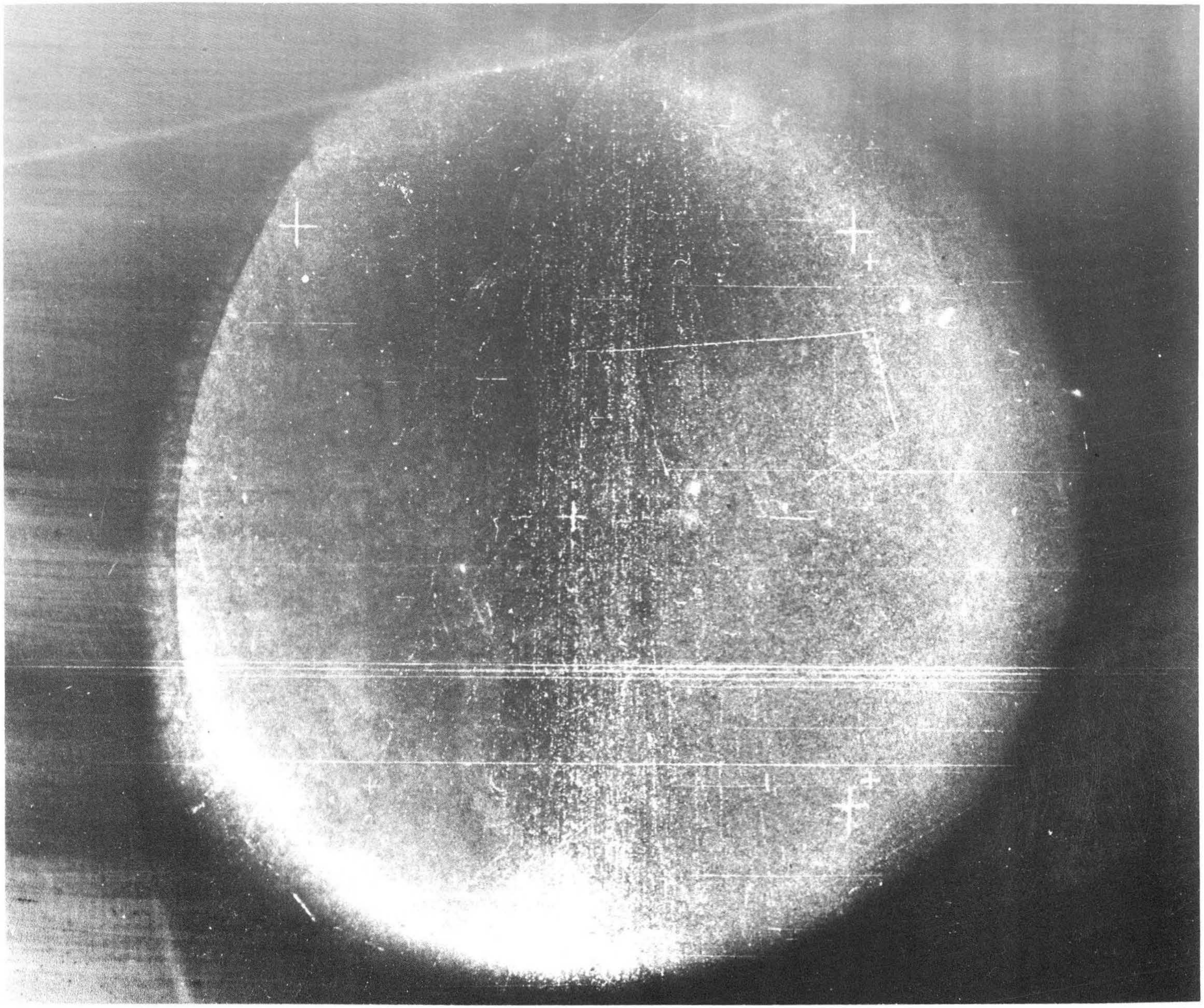

ZN-2274

Fig. 8.

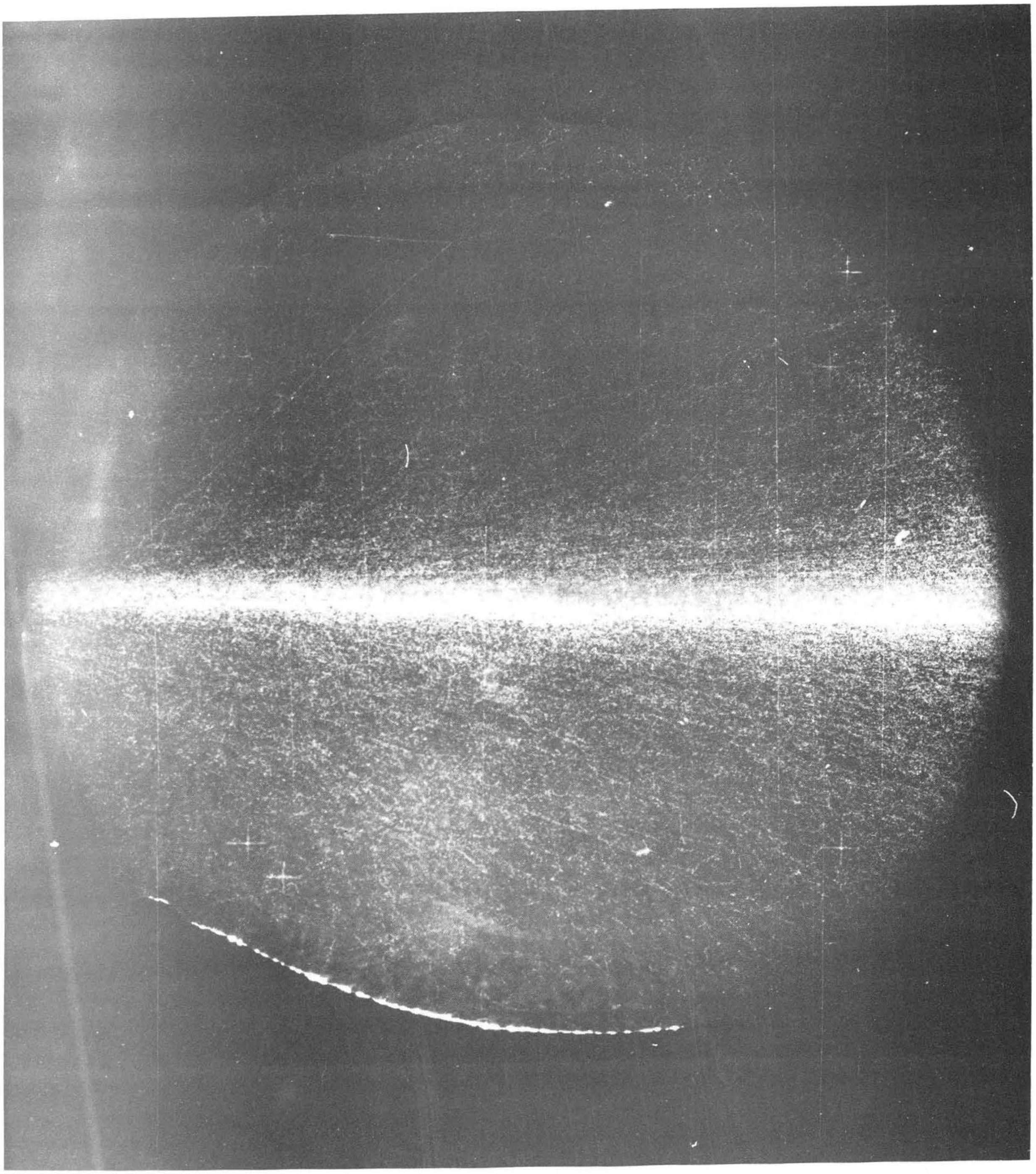

ZN-2275

Fig. 9.